Generation of Smooth and Accurate Surface Models for Surgical Planning and Simulation

Tobias Moench[a], Mathias Neugebauer[a], Peter Hahn[b] and Bernhard Preim[a,b]

[a]Department of Simulation and Graphics, Otto-von-Guericke University Magdeburg, Germany
[b]Dornheim Medical Images, Magdeburg, Germany

ABSTRACT

Surface models from medical image data (intensity, binary) are used for evaluating spatial relationships for intervention or radiation treatment planning. Furthermore, surface models are employed for generating volume meshes for simulating e.g. tissue deformation or blood flow. In such applications, smoothness and accuracy of the models are essential. These aspects may be influenced by image preprocessing, the mesh generation algorithm and mesh postprocessing (smoothing, simplification). Thus, we evaluated the influences of different image preprocessing methods (Gaussian smoothing, morphological operators, shape-based interpolation), model generation (Marching Cubes, Constrained Elastic Surface Nets, MPU Implicits) and mesh postprocessing to intensity and binary data with respect to its application within surgical planning and simulation. The resulting surface meshes are evaluated regarding their smoothness, accuracy and mesh quality. We consider the local curvature, equi-angle skewness, (Hausdorff) distances between two meshes (before and after processing), and volume preservation as measures. We discuss these results concerning their suitability for different applications in the field of surgical planning as well as finite element simulations and make recommendations on how to receive smooth and accurate surface meshes for exemplary cases.

Keywords: Mesh generation, accuracy, smoothness, surgical planning, simulation

1. INTRODUCTION

Patient-specific medical surface models are used to convey the morphology of anatomic and pathologic structures as well as spatial relations between them. Moreover, surface models are essential for generating volume models for simulations where the blood flow or the behavior of tissue is simulated. The surface meshes are reconstructed from volume data, e.g. from computed tomography (CT) or magnetic resonance imaging (MRI). The structures need to be identified and delineated by user interaction (e.g. manual segmentation), automatic or semi-automatic approaches. Thus, the generation of surface models from medical image data is a multi-stage process including segmentation and preprocessing of relevant structures, mesh generation and mesh postprocessing (e.g. simplification, smoothing, remeshing). An inherent problem of medical image data is the limited resolution and the anisotropic character of the voxels (slice thickness is usually considerably larger than the in-plane resolution). Thus, the surface meshes may contain several artifacts, such as staircases, terraces, holes, and noise. In medical visualization, these models should look naturally, referring to smoothness of the surface, since anatomical structures usually do not exhibit sharp edges. A natural appearance is particularly desired by surgeons, since it resembles the intraoperative experience. The artifacts represent strong differences compared to the original structure and influence the visual and numerical evaluation of spatial relationships. For surgical planning it is essential to employ accurate models to ensure the correct computation and visualization of safety margins and potential infiltrations. Accuracy can therefore be regarded as preservation of volume and shape of the individual structures but also as preservation of distances between relevant neighboring structures. Within other applications, such as computational fluid dynamics (CFD) and simulation of tissue deformation, smooth and accurate surface models are required to enable convergence of numerical simulation. The number and quality (size and shape) of the triangles affect the accuracy of numerical computations on medical data. Triangles with bad ratios of minimum and maximum angles and strong differences in size of the triangles will prevent convergence of the

Further author information:
Tobias Moench: E-mail: moench@isg.cs.uni-magdeburg.de, Telephone: +49 (0)391 67 19359

underlying equations and lead to interpolation errors. Hence, the generation of smooth, uniform and accurate triangle meshes is desirable.
However, there are methods available to solve the specific problems, but recommendations on how to parametrize, combine and apply them to medical image data for surgical planning and simulation are missing. The influence of mesh postprocessing (smoothing) has been examined,[1] but the effects of filtering or resampling of binary masks on the accuracy of the resulting surface models are not clearly documented. Hence, we selected common preprocessing methods (image smoothing, morphological operators, shape-based interpolation) and applied them to binary masks of anatomical structures. We evaluated their influence on accuracy of the surface models and discuss the suitabilty for simulation purposes. Furthermore, we investigated the influence of different mesh generation algorithms with subsequent mesh postprocessing (smoothing, remeshing) to allow for general suggestions on mesh generation pipelines.

2. DATA AND RELATED WORK

In medical visualization, input data for model generation are intensity data (e.g. derived from computed tomography (CT) or magnetic resonance imaging (MRI)) or binary masks of the same data. However, both may introduce problems to the model generation process. In the following, we characterize these data and discuss aspects related to the mesh generation pipeline (image preprocessing, model postprocessing).

2.1 Binary and Intensity Data

Binary masks are derived from medical volume data by preprocessing and segmenting the target structures (e.g. bones, vessels, liver, lymph nodes, ...) resulting in binary images which can be transformed into a surface mesh using e.g. the Marching Cubes (MC) algorithm,[2] Constrained Elastic Surface Nets (CESN),[3] or level-set methods.[4] Binary segmentation removes all intensity information from the image data and reduces the structures to voxels classified as object and background. Unfortunately, depending on the model generation algorithm, binary segmented image data may introduce additional artifacts (e.g. staircases, terraces, frayed parts or holes) to the final model which can be reduced by suitable preprocessing of the segmentation masks (e.g. increasing the resolution by interpolation, smoothing, morphological operators) or subsequent mesh postprocessing (smoothing). Alternatively, the Constrained Elastic Surface Nets (CESN) method combines reconstruction and iterative smoothing (forcing the surfaces nodes to remain within their original cells). This can be compared to a MC surface mesh with consecutive (node position restricted) laplacian smoothing. CESN guarantees a certain smoothness reducing terracing artifacts but retaining features, but larger terraces may still remain to the model. Very thin structures (diameter <= voxel size, e.g. blood vessels) tend to collapse to a line.
Applying surface reconstruction methods, such as the MC algorithm, to non-binary data is promising but may still not remove all critical artifacts reliably. Mesh generation from intensity data can be a difficult task which can be facilitated by knowledge on the intensity range or shape information. The specification of an appropriate isovalue can avoid small staircases. However, intensity inhomogeneities along the borders of the structures (e.g. due to non-uniform distribution of contrast agent in vessels during image acquisition) and similar intensity values of adjacent structures will lead to wrongfully included or excluded parts (see Fig. 1). Thus, larger terraces caused by anisotropic voxels may still remain to the final model.
Involving additional information (e.g. on the expected shape) can help to overcome such identification problems. A promising example for direct mesh generation from intensity data are 3D stable mass-spring models,[5] since the model initially represents an average shape of the target structure without voxelization-related artifacts that iteratively adapts to the real data. Size and number of triangles depend on the initial model and are chosen appropriately. Important (small) features can still be detected and extracted as long as they are included in the model. Unfortunately, due to their aberrant shape, pathological structures can typically not be reconstructed such that the methods can not be used generally.
The application of general mesh generation methods to fine, elongated, and branching objects (e.g. vasculature, bronchial trees) often gives unsatisfying results with strong artifacts and thin branches collapsing to lines. Specialized methods, such as Convolution Surfaces[6] or MPU Implicits,[7] lead to an improved visual quality at the expense of a higher computational effort but might be a better choice for small and elongated structures (e.g. vasculature, bronchial trees, thin bondes) where the structure's main axis is unfavorable with respect to the slice

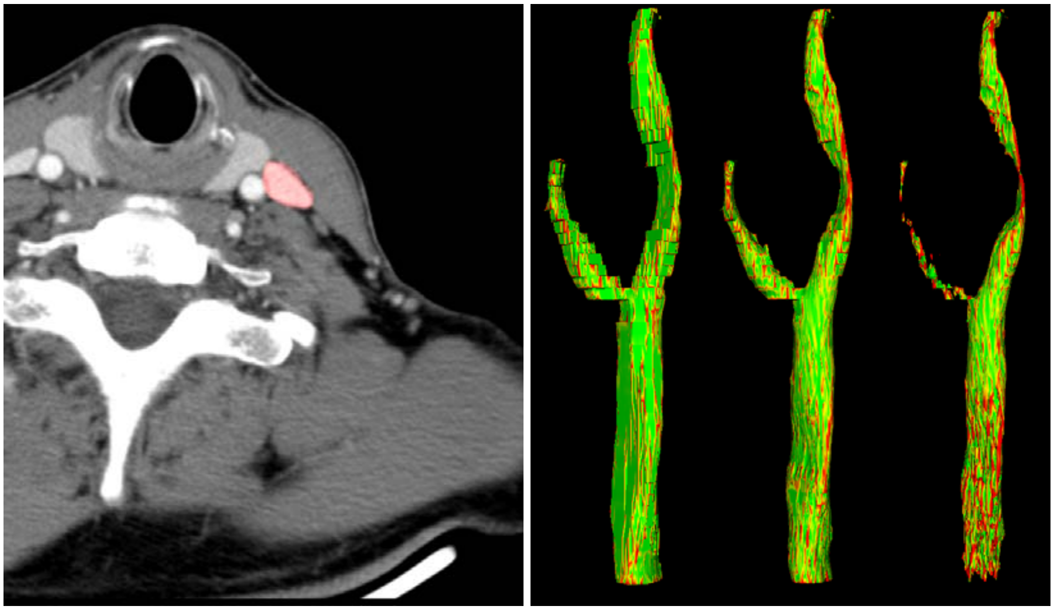

Figure 1. The figures show the intensity data (left) of a neck CT dataset overlayed with the dilated binary mask of the arteria carotis. The different 3D models show the vascular structure generated via MC from a CT dataset (masked with the dilated segmentation mask, colored red) with increasing isovalues from left to right. Volume, smoothness and artifacts are strongly affected by intensity inhomogeneities, such that the result is often a tradeoff between staircase artifacts or frayed/missing parts.

direction.
Combining the information of intensity and binary data can increase accuracy and robustness of mesh generation. Masking the intensity data with a dilated or eroded binary segmentation can prevent from involving or removing too many voxels by mistake and therefore restrict surface extraction to a certain error level. However, this can also not completely prevent from terracing artifacts, and further mesh postprocessing should be considered. Alternatively, subsequent adjustment of the surface using gradient information from the image data as presented by Bruin et al.[8] is also feasible, since accuracy and smoothness can be improved compared to the original CESN method.

2.2 Image Preprocessing

For the reduction of the mentioned problems, a wide range of methods is provided by image processing. To account for artifacts from highly anisotropic voxels, increasing the resolution in slice direction using shape-based interpolation[9] is often applied to the image data. Different interpolation methods affect smoothness, but also accuracy of the models resulting from mesh generation. Smoothing operators (e.g. Gaussian smoothing, diffusion filters) are usually employed to reduce noise within structures. They might also improve smoothness of the surface and thus reduce segmentation artifacts. However, smoothing filters are usually applied to intensity data to reduce noise within the structures preserving the borders (e.g. anisotropic diffusion). Additionally, small holes or noisy voxels at the segmentation borders can also be removed using morphological operators (opening and closing). However, manipulation of the image data might cause strong changes regarding accuracy of the final models.

2.3 Model Postprocessing

Irrespective of the input data and the mentioned visual artifacts, surface reconstruction often results in large numbers of small and possibly badly shaped (elongated) triangles. Especially within finite element method (FEM) simulations, size, shape and number of surface elements are relevant. As a consequence of anisotropic voxels the triangles often tend to be elongated decreasing the overall mesh quality and simulation accuracy.

Thus, simplification and remeshing steps[10] are necessary to meet the requirements of performance and numerical computations (e.g. using quadric error metrics[11]). Besides resolution, the quality of the triangles affects interpolation steps in simulations of e.g. blood flow in CFD.[12] The MC algorithm may additionally raise problems due to ambiguities (see also[13]) and will not remove any possible artifacts.

Noise, staircase artifacts, or plateaus resulting from the limited resolution can be removed by appropriate mesh smoothing operations reducing the local curvature (e.g. Dual Marching Cubes,[14] Laplace filter, Laplace+HC,[15] Mean Curvature Flow,[16] or Taubin's $\lambda|\mu$(LowPass) smoothing[17]). Many of the related methods focus on the removal of noise,[15,18] which arose e.g. as an artifact of laser scanning and have not been applied to medical data.[16,19] Especially Belyaev et al.[19] compared mesh smoothing approaches by adding noise to a perfect artificial reference mesh and subsequently smoothed it. Similarly, Desbrun et al.[16] focus on the treatment of noise and uneven edges using diffusion and curvature flow. Furthermore, the preservation of sharp edges does not fit to the application on medical data because of anatomical structures typically having smoother shapes. Bade et al.[20] compared different smoothing algorithms for models derived from binary segmentation masks but did not involve intensity information, neither for initial model generation nor during surface enhancement. Furthermore, they presented a smoothing constraint to preserve accuracy during mesh filtering.[1]

2.4 Requirements

Obviously, medical image data exhibits further artifacts which need to be reduced for optimally supporting surgical planning, intervention planning, CFD or tissue simulation where anatomical structures need to be displayed or simulated faithfully. The requirements to be considered by the model generation pipeline can be summarized as follows:

- The generated surface should represent the object boundary as close as possible.
- Distances between neighboring structures might not be changed.
- Staircases and terraces have to be reduced or removed as they are caused by discretization and segmentation and do not represent the typical shape of anatomical structures.
- Sharp edges should be avoided, since anatomical structures do not exhibit such surface shapes (in contrast to CAD).
- Remaining artifacts should not be emphasized by the mesh generation algorithm.
- Frayed parts (caused by over-/undersegmentation) have to be removed or reduced, since they are additional or missing parts.
- The mesh resolution has to be chosen adequately to represent the individual anatomical shape and relevant features.
- With respect to performance aspects but also numerical accuracy during simulation the mesh should not be over-/undersampled.

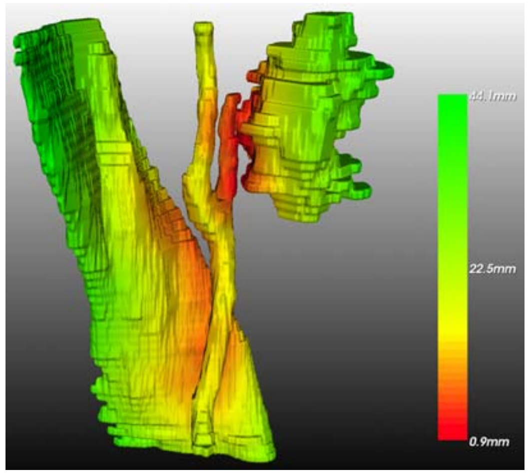

Figure 2. The figure shows the three target structures (colored by euclidean distances to each other, in mm) generated from binary masks using Marching Cubes algorithm without further pre-/postprocessing.

3. INFLUENCES OF PREPROCESSING

The preprocessing of image data can help to improve the visual quality of surface models. However, altering the image data may also have strong influences on the accuracy of the resulting 3D models.

3.1 Sample Data

We decided to apply different types of preprocessing methods to binary segmented structures of the neck. Neck surgery is a typical example where different categories of anatomic shapes are located very close to each other. We refer to three characteristic structures from a clinical CT dataset of the neck (voxel size: 0.453mm$\times$0.453mm$\times$3mm). Since the structures often exhibit similar intensity values, the selected structures have been segmented by a medical expert: (1) a vessel (arteria carotis), (2) a tumor located directly near the vessel, and (3) a muscle (sternocleidomastoid muscle, SCM) located close to both (see Fig. 2). For generating initial surface models, we employed the Marching Cubes algorithm (IsoValue=0.5$\times$MaxValue) without any mesh postprocessing. These models are used as reference data.

For artifact reduction, we increased the resolution in slice direction to isotropic voxels using shape-based interpolation (with linear, hermite spline, and cubic b-spline interpolation). 3D Gaussian smoothing (3$\times$3$\times$3 and 5$\times$5$\times$5 voxels) has been applied, since smoother boundaries in the image data should allow for smoother surfaces after reconstruction. Furthermore, morphological operators, such as dilation and erosion (spherical kernels: 3$\times$3$\times$3 and 5$\times$5$\times$5 voxels), have also been applied to remove smaller frayed parts or holes at the object boundaries. Image smoothing and morphological operators are applied to the initial segmentation masks and the resampled data.

To evaluate the influence of these methods to the mesh generation process, we considered smoothness, volume preservation and accuracy (distance preservation) of the initial and resulting surface models. Smoothness is interpreted as average maximum node curvature to show the effects on artifacts, such as staircases exhibiting high curvature values. Distance preservation is evaluated in terms of the Hausdorff distance (in relation to the specific voxel diagonal) between the initial model (generated from the original segmentation masks) and the processed models. We consider distance values of $<0.5\times$voxel diagonal as acceptable. However, in case of frayed parts or strong contour differences between neighboring slices, even stronger distance changes might be acceptable in selected cases.

3.2 Results

In terms of accuracy, our tests showed that the mesh generation process is very sensitive to the considered preprocessing methods. For all employed structures, Gaussian smoothing could slightly reduce the overall maximum

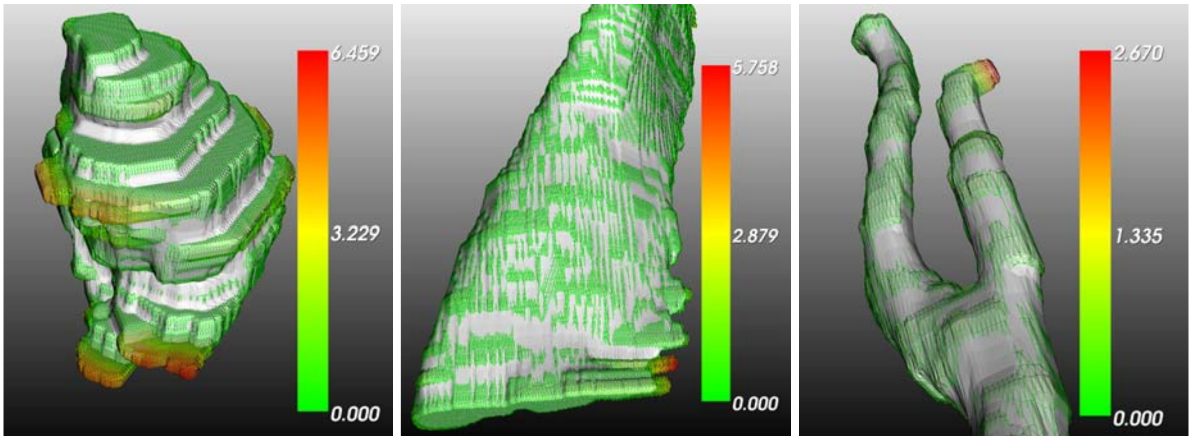

(a) Tumor (b) Sternocleidomastoid Muscle (c) Arteria Carotis

Figure 3. The three images show the surface models generated from the initial segmentation masks (colored mesh) and from image data after Gaussian smoothing (3×3×3, gray colored surface). The meshes are colored by the Euclidean distances (in mm) between each two models.

curvature (depending on kernel size, see Tab. 1), whereby accuracy decreased significantly (e.g. 2.11 and 3.21 × voxel diagonal for the tumor data). The main differences to the initial model occured where the segmentation borders show a strong variation from slice to slice (see Fig. 3(a)). In contrast, the effects of smoothing (3×3×3) to the more continuous vessel data are more acceptable (volume changes <4%, avg. max. curvature reduced by ≈28%, Hausdorff distance 0.87×voxel diagonal, see Fig. 3(c)). Looking at the results for the muscle data showed problems for parts of the structure, where there is nearly no segmentation overlap between neighboring slices (as indicated in Fig. 3(b), bottom right part of the model).

For the opening operators (both kernel sizes), nearly no volume change was noticed and the Hausdorff distance for the vessel (0.26 and 0.41× voxel diagonal) and the muscle (0.47 and 0.60× voxel diagonal) data remained low. In contrast, the tumor data with strong inter-slice variations of the segmentation borders resulted again in unacceptable inaccuracies. Closing operations caused strong volume shrinkage and thus large Hausdorff distances to the original surface model.

Resampling of the segmentation masks via shape-based interpolation achieved very good values in terms of volume preservation and accuracy for all examined anatomical structures. Curvature reduction could only be achieved by subsequent smoothing of the resampled data (see Tab. 2). Cubic B-spline interpolation yielded unacceptable distance values (≈2-3× voxel diagonal) for the tumor and muscle dataset.

4. MESH GENERATION AND POSTPROCESSING FOR SELECTED CASES

The choice of an appropriate workflow for the generation of smooth and accurate surface models depends on the data and subsequent usage of the resulting mesh. Applications, such as surgical planning, primarily require accuracy, whereas CFD or the simulation of tissue additionally involve mesh quality (shape, resolution). We selected data from two different fields to discuss and evaluate basic mesh generation and postprocessing methods with focus on the requirements specified in Section 2.4.

4.1 Neck Surgery

The neck contains a variety of close and differently shaped anatomical structures (e.g. lymph nodes, vessels, pharynx, muscels, thyroid cartilage, bones, salivary glands). Medical visualization is applied to evaluate their spatial relations (e.g. extent of a tumor and its possible infiltration to surrounding structures). Hence, accuracy regarding the distances between the structures and their exact shape and size are most important for the correct interpretation of safety margins in surgical planning. As an example, we refer again to a CT dataset (voxel size: 0.453mm×0.453mm×3mm) of the neck with a tumor located close to important vessels, such as vena jugularis

Table 1. The table shows the results for selected preprocessing methods. Distances are given as the Hausdorff distance as fraction of the original voxel diagonal compared to the reference model.

Model	Filtering	Kernel Size	Volume (%)	Avg. Max. Curvature	Distance
Tumor	none	none	100	0.44	0
	Gauss	3×3×3	97.26	0.37	2.11
	Opening	3×3×3	104.89	0.43	3.23
	Closing	3×3×3	90.06	0.43	3.47
	Gauss	5×5×5	96.55	0.31	3.21
	Opening	5×5×5	108.72	0.42	3.24
	Closing	5×5×5	82.73	0.39	3.8
Arteria Carotis	none	none	100	0.64	0
	Gauss	3×3×3	96.14	0.46	0.87
	Opening	3×3×3	102.20	0.63	0.26
	Closing	3×3×3	90.62	0.61	1.46
	Gauss	5×5×5	93.49	0.42	1.06
	Opening	5×5×5	104.44	0.62	0.41
	Closing	5×5×5	78.82	0.61	2.29
SCM	none	none	100	0.52	0
	Gauss	3×3×3	98.97	0.30	1.88
	Opening	3×3×3	100.85	0.50	0.47
	Closing	3×3×3	97.24	0.48	3.66
	Gauss	5×5×5	98.33	0.24	1.99
	Opening	5×5×5	101.16	0.50	0.60
	Closing	5×5×5	94.32	0.48	3.96

Table 2. The table shows the results for shape-based interpolation (hermite spline) and subsequent application of the filtering methods. Distances are given as the Hausdorff distance as fraction of the voxel diagonal.

Model	Filtering	Volume (%)	Avg. Max. Curvature	Distance
Tumor	none	99.36	0.60	0.30
	Gauss	99.17	0.41	0.35
	Opening	99.89	0.58	0.83
	Closing	98.61	0.59	0.51
Arteria Carotis	none	98.36	0.68	0.30
	Gauss	97.65	0.51	0.33
	Opening	99.62	0.66	0.30
	Closing	97.01	0.66	0.30
SCM	none	99.44	0.57	0.30
	Gauss	99.22	0.35	0.40
	Opening	100.00	0.53	0.32
	Closing	98.62	0.54	0.77

and arteria carotis.

Pathological structures, such as tumors, can usually not be identified automatically, which necessitates manual segmentations involving anatomical knowledge. We applied the MC algorithm to the binary mask of a tumor with subsequent volume preserving smoothing (Laplace+HC or Taubin's $\lambda|\mu$ filter) and additional node positioning constraints (restricting to cubical or diamond cells). This eliminates sharp artifical edges and smaller staircase artifacts but does not alter the segmented contours, which is important since especially tumors often do not exhibit completely smooth contours. As depicted in Table 3, an appropriate mesh smoothing (Laplace+HC, 10 iterations, λ=0.5, node position restricted to cubical cells) preserves the volume (99.09%), whereas the mean curvature is obviously reduced. The CESN method, which is comparable to the mentioned steps, achieves similar results and yields just a negligible volume shrinkage (97.63% volume preserved). However, the tumor model still suffers from strong terracing artifacts due to 3mm slice thickness (vs. 0.45mm in-plane resolution). A smooth model could only be achieved by very strong mesh smoothing which would evoke inacceptable inaccuracies. Since the correct spatial extent of the tumor is most important in surgical planning and the shape of pathological structures might be very irregular, preservation of shape and distances should be preferred to visual quality in that case.

Vasculature may also be hard to distinguish from surrounding tissue by analyzing the intensity values only. However, masking the intensity data with dilated binary segmentations as boundary constraint can exclude false additional or detached parts and thus allow mesh generation via MC. Subsequently applying node position constrained mesh smoothing (Laplace+HC, 10 iterations, λ=0.5) results in a smooth and accurate vessel model (see Tab. 3, 99.56% volume preservation, mean curvature reduced to 0.265) as long as the target structure does not contain filigree parts. The comparable CESN approach yields similar results regarding smoothness but suffers from stronger volume shrinkage (14.25%). For the vessel model we additionally applied MPU Implicits with oversampling of thin structures which led to a smooth and artifact-reduced model. The resulting surface model exhibits a more natural look at branching points. The curvature is reduced, but the volume increased about 5% and exhibits strong distance deviations at the structure's endings (1.15× voxel diagonal). The MPUI method yields visually better models but the required parameters are very sensitive to minimal changes and the models even tend to grow.

Comparing these methods regarding the smoothness and preservation of distances between the target structures,

	Tumor			Vena jugularis			
	MC	Smoothed MC	CESN	MC	Smoothed MC	MPUI	CESN
Volume	100%	99.09%	97.63%	100%	99.56%	105.44%	85.75%
Mean Curv.	0.505	0.366	0.422	0.451	0.265	0.222	0.301
Distance	0	0.307	0.306	0	0.359	1.150	0.742
EAS (Mean)	0.427	0.421	0.406	0.652	0.675	0.462	0.658
EAS (Max)	0.981	0.887	0.870	0.983	0.910	0.999	0.915
Homogeneity (EAS)	0.276	0.210	0.197	0.288	0.162	0.516	0.174
Homogeneity (Size)	0.182	0.104	0.089	0.234	0.126	0.828	0.141

Table 3. Comparison of the initial MC mesh of a tumor (from binary data, 48k faces) and the vena jugularis (from masked intensity data, 21k faces): smoothed MC mesh (Laplace+HC), CESN, and MPUI of the vessel (10k faces). Distances are given as the Hausdorff distance in relation to the specific voxel diagonal. Homogeneity is defined as the mean maximum error within the 1st order neigborhood of the triangles.

Tumor / Vessel	MC	Smoothed MC	CESN
MC	0.334	0.373	0.752
Smoothed MC	0.344	0.411	0.769
CESN	0.712	0.726	0.996
MPUI	0.710	0.398	0.849

Table 4. Comparison of the minimal distances between the examined structures. The values are given as fraction of the specific voxel diagonal.

a combination of MC and subsequent node position constrained smoothing gives the best results without altering the minimum distances between neighboring structures (refer to Tab. 4).
The quality of the meshes is usually not relevant for surgical planning. Due to the anisotropic voxel size, all approaches created large numbers of badly shaped, elongated triangles (EAS $\approx$0.9, see Tab. 3). Especially the MPUI approach results again in very inhomogeneous meshes. Hence, models generated from comparable data need to be completely remeshed before usage in simulation applications. But also for usage in surgical planning applications, an adjustment of the mesh resolution might be appropriate.

4.2 Simulation

The simulation of tissue deformation or of blood flow in CFD incorporates complex computations (e.g. FEMs) on volume meshes built from 3D surface models. Thus, the quality of the initial surface meshes affects the volume meshes and finally computational effort and errors. Besides the general requirements (accuracy, preservation of shape and size, smoothness), quality and homogeneity (of size and quality) become important. For example the shape of surface triangles can be described via equi-angle skewness (EAS, ranging from 0 to 1), whereas lower values of EAS represent higher mesh quality.

	MC	Smoothed MC	Smoothed MC + Optimized	CESN	MPUI
Volume	100%	100.56%	100.07%	90.37%	105.63%
Mean Curvature	0.354	0.262	0.494	0.253	0.277
Distance	0	0.197	0.320	0.514	0.768
EAS (Mean, Max)	0.322, 0.924	0.265, 0.698	0.149, 0.643	0.254, 0.701	0.462, 0.999
Homogeneity (EAS)	0.291	0.212	0.146	0.215	0.552
Homogeneity (Size)	0.145	0.109	0.013	0.095	0.208

Table 5. Comparison of the initial MC mesh (10k faces) of a cerebral aneurysm (from intensity data, 256×384×88, 0.781×0.781×0.781 mm), the smoothed MC mesh (Taubin's $\lambda|\mu$ filter), an optimized high resolution MC mesh (62k faces) and CESN (from binary data, 10k faces). Distances are given as the Hausdorff distance in relation to the specific voxel diagonal. Homogeneity is defined as the mean maximum error within the 1st order neigborhood of the triangles.

4.2.1 Blood Flow in Cerebral Aneurysms

CFD typically focuses on one single target structure. Thus, spatial relationships to neighboring structures are less relevant. The individual morphology of the cerebral aneurysm and connected vessels need to be preserved to allow for a successful computational approximation of the real blood flow behavior.
In the image data, aneurysms are represented as contrast-enhanced connected regions. Applying the MC algorithm to the intensity data (MRI angiography, voxel size: 0.781mm×0.781mm×0.781mm, no resampling) with an appropriate isovalue results in an accurate initial surface model of the aneurysm (see Fig. 4). A preceding filtering step with a dilated binary mask removes background structures and noise exhibiting similar intensities. Slight smoothing (e.g. Taubin's $\lambda|\mu$ filter, 20 iterations, λ=0.5, μ=-0.52, 1st order neighborhood) removes small staircases and fine, sharp features which could cause a locally very high subdivision during volume mesh generation for FEM. As depicted in Table 5, mean curvature is reduced by 26%, whereas volume is preserved and the maximum distance is less than 20% of the voxel diagonal (compared to the initial MC mesh).
Filigree elements with a diameter equal to the voxel size or less cannot be clearly reconstructed with the provided workflow, since the intensity values will vary strongly due to partial volume effect. If the segmentation results in binary masks, or if only binary data is available, MPU Implicits with oversampling of the filigree structures yield smooth and volume preserving surface models (see Tab. 5). Other approaches for binary data, such as CESN, shrink the volume (90.37% preserved) and should not be applied to thin vessels.
Isotropic voxel dimensions facilitate a better initial mesh quality, since the triangles do not get elongated in slice direction, whereas mesh smoothing can slightly improve the quality (e.g. EAS decreased from 0.924 to 0.698). Subdividing the surface elements during the optimization process yields a smooth and accurate high

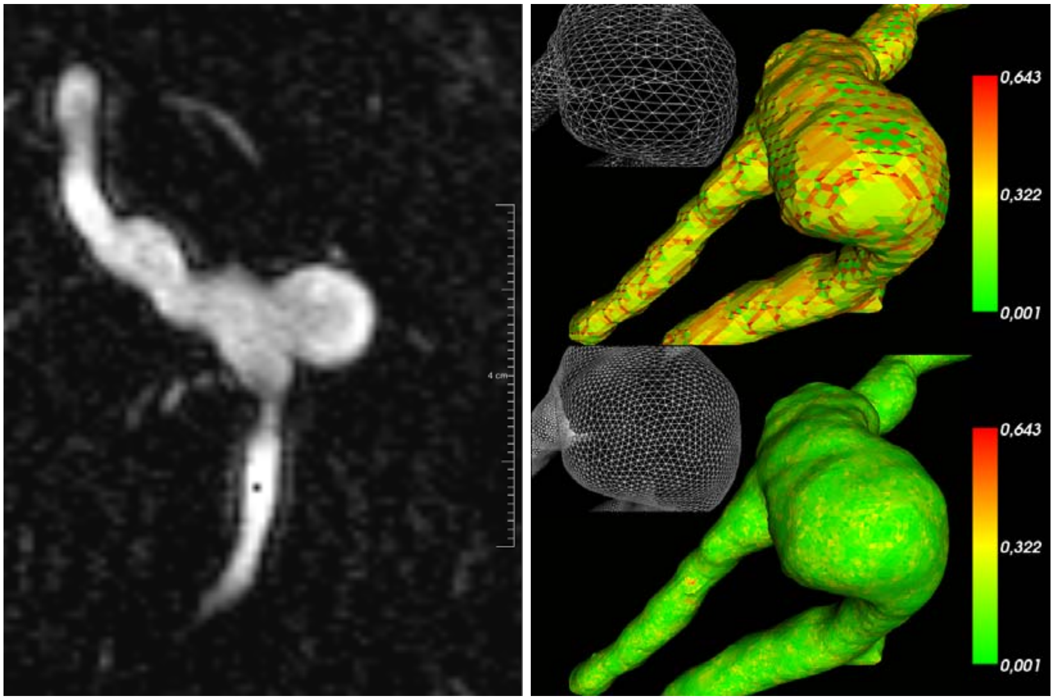

Figure 4. Surface model of a cerebral aneurysm colored by equi-angle skewness (flat shaded). Left: A sample slice of the employed MRI angiography data. Top right: Initial mesh derived from MC. Bottom right: Smoothed MC mesh (Taubin's $\lambda|\mu$ filter) after subdivision and optimization. In the top left corner of each subfigure, a corresponding close view to the mesh is given.

quality mesh. Further edge flipping and collapsing can reduce the mean EAS enormously (from 0.265 to 0.149). Moreover, these quality optimization steps go along with simplifications and may hence introduce additional errors. For example a simplification of the optimized MC mesh from 62k faces to 8k increases the Hausdorff distance to the initial MC model from 0.32 to 1.175 of the voxel diagonal. Since CFD is usually not used in performance-critical real time applications, a high mesh resolution can be accepted allowing smaller interpolation steps and hence less errors during simulation. Comparing the homogeneity of the meshes with respect to size and EAS of the triangles, MC with subsequent smoothing and CESN yield similar results, whereas the MPUI approach generates very inhomogeneous surface meshes (see Tab. 5). Optimal results can be achieved by subsequent quality focussed remeshing.

4.2.2 Tissue Deformation

The requirements for the simulation of tissue deformation can be compared to the aspects in CFD. Depending on the data, a good quality mesh can again be derived by applying the MC algorithm to (masked) intensity data with subsequent filtering using Taubin's $\lambda|\mu$ smoothing. If there is only binary data available, CESN (or an equivalent combination of MC and smoothing with node positioning constraint) should be used for reconstruction, since the mesh is slightly smoothed but still prevented from strong volume shrinkage (see Fig. 5 for an example of the liver).

The required level of detail is the main difference to CFD simulations. Since tissue deformation is typically used in interactive visualization environments, rendering performance and simulation speed are the most important aspects. Edge flipping and collapsing techniques decimate the mesh, but reduce accuracy, whereas a good quality of the mesh needs to be guaranteed (e.g. using quadric error metrics).

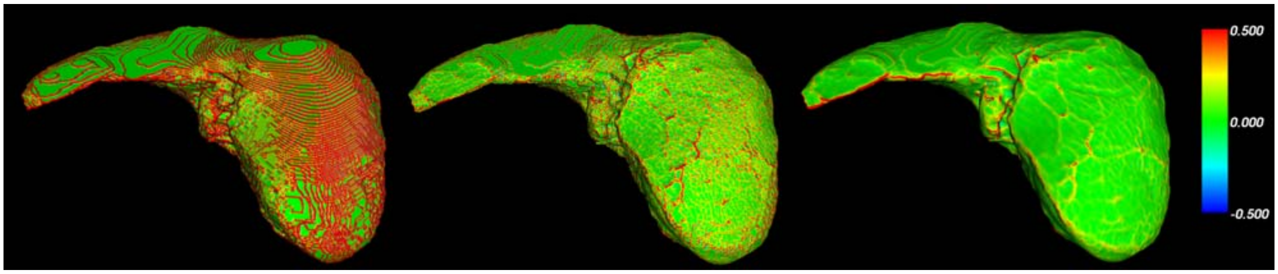

Figure 5. Surface model of a liver colored by mean curvature: MC applied to binary mask (left), to masked and smoothed non-binary data (middle), and CESN applied to binary data (right).

5. CONCLUSION

The suitability of mesh generation methods for medical image data is influenced by several aspects, such as the goal in diagnosis or treatment planning, data resolution, voxel size, or shape information. We considered several steps of the mesh generation pipeline with respect to accuracy and focussed on the influence of image preprocessing but also of mesh generation and postprocessing for different applications.

We showed that basic image preprocessing methods can improve visual quality of the final models but can also have strong influences on distances between neighboring structures and thus may be critical for application within a surgical context. A commonly used technique to overcome terracing artifacts by image preprocessing is the interpolation of additional slices. However, accuracy of the results strongly depends on the involved interpolation method.

The choice of an appropriate mesh generation method (e.g. MC, CESN, MPUI) depends on the type of available data. We tested commonly used mesh generation algorithms (MC, CESN) in combination with appropriate constrained smoothing (Laplace+HC, Taubin's $\lambda|\mu$) and optimization steps (edge flipping and collapsing) and showed that they are applicable for the fields of surgical planning and simulation for intensity and binary data. The discussed approaches yield adequate surface models for most relevant structures, except thin elongated objects where more specialized methods need to be applied. Especially for pathological structures, the mesh generation process should focus more on accuracy than on smoothness.

However, it is important to involve more data and structures of the same categories and thus evaluate the influence of different structure sizes and diameters (e.g. for vascular structures). Further methods involving intensity information need to be considered to increase accuracy compared to voxel-cell-restricted approaches. For example model-based methods, such as stable mass-spring models, can be applied to structures exhibiting typical shape information and characteristic gradients at the boundaries (e.g. lymph nodes, thyroid cartilage). Since the mass-spring model's nodes are not restricted to initial voxel cell boundaries, the method is able to fit target structures without introducing terracing artifacts and thus to yield more accurate results. Additionally, the adjustment of visual smoothness could help to provide naturally looking surface models without altering the topology too much.

ACKNOWLEDGMENTS

Tobias Moench is funded by the German Ministry of Education and Science (BMBF) within the ViERforES project (http://vierfores.de, no. 01IM08003C).

REFERENCES

[1] Bade, R., Konrad, O., and Preim, B., "Reducing artifacts in surface meshes extracted from binary volumes," *Journal of WSCG* **15**(1-3), 67–74 (2007).

[2] Lorensen, W. E. and Cline, H. E., "Marching cubes: A high resolution 3d surface construction algorithm," in [*Proceedings of the ACM SIGGRAPH Conference on Computer Graphics*], 163–169 (1987).

[3] Gibson, S. F. F., "Constrained elastic surface nets: Generating smooth surfaces from binary segmented data," in [*MICCAI '98: Proceedings of the First International Conference on Medical Image Computing and Computer-Assisted Intervention*], 888–898, Springer-Verlag, London, UK (1998).

[4] Whitaker, R. T., "Reducing aliasing artifacts in iso-surfaces of binary volumes," in [*VVS '00: Proceedings of the 2000 IEEE symposium on Volume visualization*], 23–32, ACM, New York, NY, USA (2000).

[5] Dornheim, J., Seim, H., Preim, B., Hertel, I., and Strauss, G., "Segmentation of neck lymph nodes in ct datasets with stable 3d mass-spring models," in [*Proceedings of Medical Image Computing and Computer-Assisted Intervention (MICCAI)*], *Lecture Notes in Computer Science*, 478–485, Springer (2006).

[6] Oeltze, S. and Preim, B., "Visualization of Vascular Structures: Method, Validation and Evaluation," *IEEE Transactions on Medical Imaging* **24**, 540–548 (April 2005).

[7] Schumann, C., Oeltze, S., Bade, R., and Preim, B., "Model-free surface visualization of vascular trees," in [*IEEE/Eurographics Symposium on Visualization, Eurographics*], 283–290 (2007).

[8] Bruin, P. W. D., Vos, F. M., Post, F. H., Frisken-Gibson, S. F., and Vossepoel, A. M., "Improving triangle mesh quality with surfacenets," in [*Proceedings of Medical Image Computing and Computer-Assisted Intervention (MICCAI)*], 804–813 (2000).

[9] Raya, S. and Udupa, J., "Shape-based interpolation of multidimensional objects," *IEEE Transactions on Medical Imaging* **9**(3), 32–42 (1990).

[10] Hoppe, H., Derose, T., Duchamp, T., Mcdonald, J., and Stuetzle, W., "Mesh optimization," *Computer Graphics* **27**(Annual Conference Series), 19–26 (1993).

[11] Garland, M. and Heckbert, P. S., "Surface simplification using quadric error metrics," in [*Proceedings of the ACM SIGGRAPH Conference on Computer Graphics*], 209–216 (1997).

[12] Shewchuk, J. R., "What is a good linear element? interpolation, conditioning, and quality measures," in [*Proceedings of the 11th International Meshing Roundtable*], 115–126 (September 2002).

[13] Allamandri, F., Cignoni, P., Montani, C., and Scopigno, R., "Adaptively adjusting marching cubes output to fit a trilinear reconstruction filter," in [*EG Workshop on Scientific Visualization '98*], 25–34 (1998).

[14] Nielson, G. M., "Dual marching cubes," in [*VIS '04: Proceedings of the conference on Visualization '04*], 489–496, IEEE Computer Society, Washington, DC, USA (2004).

[15] Vollmer, J., Mencl, R., and Müller, H., "Improved laplacian smoothing of noisy surface meshes," *Computer Graphics Forum* **18**(3), 131–138 (1999).

[16] Desbrun, M., Meyer, M., Schröder, P., and Barr, A. H., "Implicit fairing of irregular meshes using diffusion and curvature flow," in [*Proceedings of the ACM SIGGRAPH Conference on Computer Graphics*], 317–324, ACM Press/Addison-Wesley Publishing Co., New York, NY, USA (1999).

[17] Taubin, G., "A signal processing approach to fair surface design," in [*Proceedings of the ACM SIGGRAPH Conference on Computer Graphics*], 351–358, ACM, New York, NY, USA (1995).

[18] Tasdizen, T. and Whitaker, R., "Anisotropic diffusion of surface normals for feature preserving surface reconstruction," in [*Proceedings of Fourth International Conference on 3-D Imaging and Modeling*], 353–360 (October 2003).

[19] Belyaev, A. and Ohtake, Y., "A comparison of mesh smoothing methods," in [*Proceedings of the Israel-Korea BiNational Conference on Geometric Modeling and Computer Graphics*], 83–87 (2003).

[20] Bade, R., Haase, J., and Preim, B., "Comparison of fundamental mesh smoothing algorithms for medical surface models," in [*Simulation und Visualisierung (2006)*], 289–304 (2006).